

FATIGUE CRACK PROPAGATION PROPERTIES IN CORROSION RESISTANT WELDED JOINTS

Geraldo de Paula Martins*

*Nuclear Technology development Center
Brazilian National Commission of Nuclear
Energy*

*Rua professor Mário Werneck, s/nº
Pampulha, Belo Horizonte, MG, Brasil*

*Tel.: 55-31-34993332; Fax: 55-31-
34993390*

E-mail: gpm@cdtn.br

Carlos Alberto Cimini Jr.

*Federal University of Minas Gerais
Mechanical Engineering Department,
Pampulha, Belo Horizonte, MG. CEP
30123-970. Tel.: (31) 3499-5239; E-mail:
cimini@demec.ufmg.br*

Leonardo Barbosa Godefroid

*Federal University of Ouro Preto
Department of Metallurgy
Ouro Preto, MG Brazil. CEP 35400-000*

Emerson Giovanni Rabello

*Nuclear Technology development Center
Brazilian National Commission of Nuclear
Energy*

ABSTRACT

Fatigue crack growth resistance properties are obtained through fatigue crack propagation tests. The results, obtained from a log-log plot presents three regions: region I, where the microstructure, mean stress and environment have a high influence. Region II, that presents a linear behavior and region III where the material reaches the fracture toughness and results in an instable fracture. In this work it is studied the behavior of corrosion resistant USI SAC 50 steel welded joints, using compact tension specimens with notch localized on the base metal, heat affected zone and melted zone. It is obtained stable crack propagation equations type Paris equation for the region II, with 95% confidence limit. It is observed that the heat-affected zone presents a major scatter.

Keywords: Fatigue crack propagation; heat affected zone; welded joints; fracture; fatigue

1. INTRODUCTION

The purpose of this work is to study fatigue crack propagation properties in Sac 50 steel welded joints. This study is here realized from fatigue crack propagation results. With the obtained results the Paris equation coefficients and exponents are determined for the three regions (BM, HAZ and MZ), with 95% of confidence, from regression analysis. The fracture property characterization of SAC 50 steel obtained in this work will be of very utility for support in project that uses this material. At this moment there are few works in the literature about SAC 50 steel and it implies on the necessity of tests to obtain the properties that will be used in calculus or to arbitrate the correspondent values based in materials approximately equivalents. The fatigue crack propagation resistance properties of welded joints from the refereed steel will can utilized by the users, allowing a major confidence relatively to projects of structures and components manufactured with this material and allowing the utilization of these equation to determine the remaining life with a major confidence on the results

2. FATIGUE

Fatigue Fracture is, in general, considered the most serious type of fracture in part of machines or structures. It is because the fatigue fracture can occur in service, without excessive overloads and under operational normal conditions.

Crack extension can occur with the stress intensity factor lower than K_{IC} . On this case, it is said that there is subcritical crack growth. Fatigue crack growth is an example of subcritical crack growth. Another example is stress corrosion cracking. On this work it will be presented only fatigue crack growth.

2.1 The Nature of Fatigue

The American Society for Testing and Materials (ASTM E 1823) defines Fatigue as the process of progressive localized permanent structural change occurring in a material subjected to conditions that produces fluctuating stresses and strains at some point or points and that may culminate in cracks or complete fracture after a sufficient number of fluctuations. Examples of de component that suffer the fatigue phenomenon are: automobile at the highway, airplanes in air, landing and take-off, bridges submitted to the vehicles in movement, nuclear reactors, between others.

A fatigue crack can nucleate and propagate to fracture. The number of cycles required to start a fatigue crack, is called fatigue crack life initiation, N_i . The number of cycles required to propagate a fatigue crack to a critical size is denominated fatigue crack propagation life, N_p . The total fatigue life N_t is the sum of the initiation life and propagation life, that is, (Barson and Rolfe, 1999):

$$N_t = N_i + N_p \quad (2.1)$$

There are not a defined delimitation between fatigue crack initiation and propagation. The fatigue crack initiation phenomena results in a plastic deformation process. The experience shows that, in general, the crack starts in regions of plastic deformation concentration.

The fatigue fracture process in a specimen or in a part can be divided in three phases:

Phase I: crack initiation (tangential stress). On the phase I the crack initiate at the surface and propagate at a defined crystallographic direction. The length crack at this stage is essentially controlled by shear stress. The cyclic sollicitation move the dislocations, that form persistent slip bands, generating intrusions and extrusions resulting to micro-cracks formed by punctual plastic (Suresh, 1998).

Phase II: propagation (normal stresses). The phase II is caricaturized by a crack propagation, first, in a direction, perpendicular to the major principal stress direction, where the transition from phase I to phase II is marked by a reduction of the shear stress and a increase of the normal stress (Suresh, 1998).

Phase III: final fracture. With the increase of the normal stress, it attains the critical value of fracture toughness of the material and the crack propagates suddenly to the fracture.

The ductile crystalline materials deform, in general, by slip dislocations in crystallographic planes of high atomic density and in maximum atomic density directions. A particular aspect of the cyclic deformation region is the formation of persistent slip bands (PSB) that can be observed over a fatigue specimen surface polished in advance. Researches have explained that the PSB concentrate the major part of the plastic deformation regime. The structure associated to the PSB is a structure composed with dislocation barriers regularly spaced among then, those presents, at the interior, a major free space to permit the movement of the dislocations relative to the structure associated to the matrix. Then, this type of structure supports the plastic deformation concentration at his interior (Suresh, 1998).

During the cyclic deformation, due the intense slip dislocations inside the crystallographic plans, intrusions and extrusions with microscopic dimensions regularly spaced among then, in posterior stages can give origin to fatigue microcracks. At the absence of stress concentration of geometric nature that can originate the formation of cracks, three sites of crack initiation can be considered: the PSB, the grain boundary and the nonmetallic or intermetallic inclusions near to the surface (Anderson, 1995).

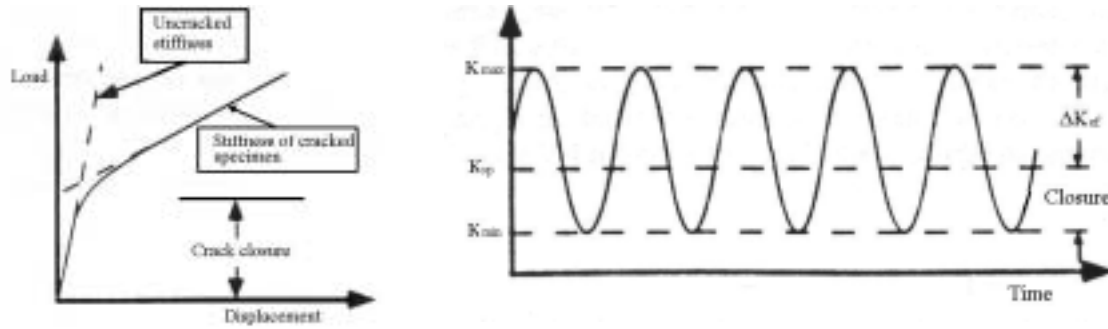
2.2 The Treshold Crack Growth

The threshold crack growth, ΔK_{th} , is defined as the inferior limit of ΔK , bellow that do not occur crack growth. In practical terms, ΔK_{th} is defined as the cyclic stress intensity factor were crack growth rate is equal to 10^{-8} mm/cycle.

Several parameters have influence on the ΔK_{th} , among then, the yield point, the grain size, microstructural elements, the mean stress, the ratio R, load history, residual stresses, the tip crack opening, the Young modulus, temperature and environment. Among these variables, the stress ratio seems the more important factor that affects the magnitude of ΔK_{th} .

2.3 Crack Closure

In 1970, Elber proposed a concept associated with fatigue crack growth (Anderson, 1995). He observed anomaly at the elastic compliance of several fatigued materials, as can be observed on Fig. 2.1.



(a) Load displacement behavior

(b) Definition of effective stress intensity range

Figure 2.1: Crack closure during fatigue crack growth; (a) crack faces are in contact at a positive load; (b) driving force reduced for fatigue, ΔK_{eff}

For elevated loads the compliance $d\Delta/dP$ corresponds with the behavior anticipated by the fracture mechanics for several specimens. However, for small loads, the compliance of the cracked specimen approaches to the compliance of a non-cracked specimen. Elber concluded that such change on the compliance was due to the contact between the crack surfaces, that is, due to the crack closure, for small cracks, but positive. Elber supposed that the crack closure reduces the crack growth rate, through the reduction of the effective stress intensity factor. Concerning to Fig. 2.20, it is observed that when a specimen is loaded between K_{max} e K_{min} , the crack surfaces are in contact at values bellow of K_{op} (stress intensity factor for crack opening). Elber assumed that the portion of the fatigue cycle bellow of K_{op} not contribute to the crack growth. Then He has defined an effective stress intensity factor ΔK_{eff} as:

$$\Delta K_{eff} = K_{max} - K_{min} \quad (2.2)$$

$$U = \frac{\Delta K_{eff}}{\Delta K} = \frac{K_{max} - K_{ab}}{K_{max} - K_{min}} \quad (2.3)$$

He had proposed an equation modified of the Paris and Erdogan equation, Eq. 2.4

$$\frac{da}{dN} = C(\Delta K_{eff})^n \quad (2.4)$$

U is defined for $K_{min} < K_{op}$. When $K_{min} \geq K_{op}$, $U = 1$, and the closure has not influence on the results. This is obtained from the value $R = 0,7$ because for $K_{min} = K_{op}$, $U=1$.

It was proposed other expressions of U to correct the crack closure in steels type, IS-1020 some of then are presented to follow (Madox, 1978):

$$C_f = \frac{\sigma_{op}}{\sigma_{max}}; \text{ and } U = 0,75 + 0,25 R \quad (2.5)$$

where σ_{op} is the opening stress (or closure); Kumar and Singh (1995) proposed the following expression for U (ferritic steels):

$$U = 0,7 + 0,15 R (2 + R) \quad (2.6)$$

2.4 Fatigue Crack Propagation

The fatigue crack propagation uses the fracture mechanics concepts, in particular, the stress intensity factor band described to follow.

Consider a throughout crack, in a plate submitted to a remote stress that varies cyclically between maximum and minimum constant values, that is, by fatigue load. Bellow is presented some definitions employed in fatigue. Referring to Fig. 2.2.

It can be defined:

$$\text{Stress range: } \Delta\sigma = \sigma_{\max} - \sigma_{\min} \quad (2.6)$$

$$\text{Stress intensity factor range: } \Delta K = K_{\max} - K_{\min} = \Delta\sigma\sqrt{\pi a} f\left(\frac{a}{W}\right) \quad (2.7)$$

$$\text{Stress amplitude: } \sigma_a = \frac{\sigma_{\max} - \sigma_{\min}}{2} \quad (2.8)$$

$$\text{Mean stress: } \sigma_m = \frac{\sigma_{\max} + \sigma_{\min}}{2} \quad (2.9)$$

$$\text{Stress ratio } R = \frac{\sigma_{\min}}{\sigma_{\max}} \quad (2.10)$$

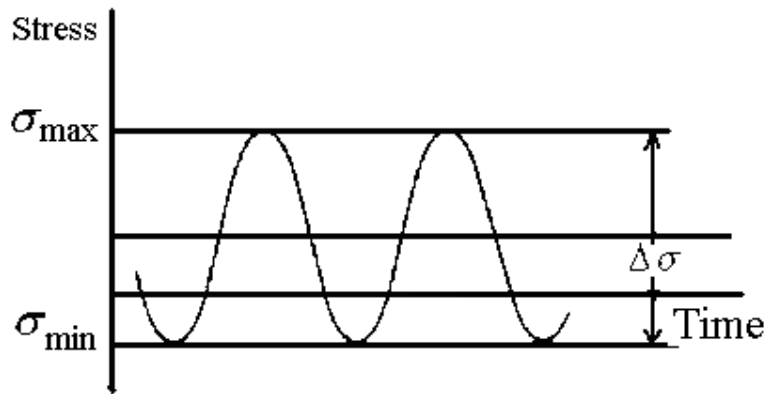


Figure 2.2: Parameters of fatigue cyclic stress with constant amplitude

If $R = -1$, it is said that the stress are reversed and it has: $\sigma_{\min} = -\sigma_{\max}$.

The fatigue crack propagation rate is defined as the ratio between the crack extension, Δa , and the number of cycles, ΔN , that is, $\Delta a/\Delta N$, and at the limit, da/dN

$$\lim_{\Delta N \rightarrow 0} \frac{\Delta a}{\Delta N} = \frac{da}{dN} \quad (2.11)$$

When the ratio stress $R = \sigma_{\min}/\sigma_{\max}$ is the same, then ΔK correlate crack propagation rate in specimens with different stress range and crack length, and specimens of different geometry, that is:

$$\frac{da}{dN} = f(\Delta K, R) \quad (2.12)$$

For fatigue crack propagation with constant amplitude, several equations have been proposed. These equations describe the behavior that involves constants of the material, load rate and the level of acting stress. The most used is the Paris equation, valid at the region II of the da/dN versus ΔK graph, to follow. Paris (1961), and Paris and Erdogan (1960) were the first to discover a relationship type power law, to describe the fatigue crack growth, at region II. The proposed relationship by them is empirical as presented bellow; C and n are constants of the material, experimentally determined:

$$\frac{da}{dN} = C(\Delta K)^n \quad (2.13)$$

3. MATERIALS AND METODOLOGY

3.1 Material

The material use on this work is the structural steel employed in civil buildings, metallic bridges, and several other applications, USI-SAC 50, 12 mm in thickness supplied by USIMINAS in form of plates de with dimensions 1000 mm X 300 mm, respectively beveled in V and 1/2 V, that were machined out at the dimensions 500 mm X 150 mm. On the Tab. 3.1 it is presented the chemical compositions of the material, supplied by the manufacturer.

Table 3.1: Chemical composition of SAC-50steel, 12 mm in thickness, supplied by the manufacturer

Thickness (mm)	Elements (% em peso)										
	C	Mn	Si	P	S	Al	Cu	Nb	Ti	Cr	Ni
12	0,12	1,13	0,34	0,024	0,013	0,037	0,26	0,022	0,009	0,44	0,20

3.2 Elaboration of the Welded Joints

The welds were carried out by the GMAW process, bevel in V and 1/2 V. The welding procedure according EPS n° MC 7622 supplied by Usiminas Mecânica, were:

Type of bevel: V, angle 45° and 22,5 in each part f the joint; and 1/2 V, angle 45° in each part of the joint; back gouging: 2 mm; gap: 3 mm;

Number of passes: 06.

Welding parameters:

Tension: 20 V for all passes;

Current: 110 A for the first pass; 220 A, for the other passes;

Electrode: AWS E 7018G, diameter 3,25 mm for the first pass and diameter 5 mm for the remainders five passes.

Welding speed: 300 mm/min

For the welding with bevels V and 1/2 V, the parameters were the same, as the number of passes. It was applied a minimum pre-heating of 323 K (50°C) and maintained a minimum temperature between passes of 323 K (50°C), with grinding between passes for removal the slag. The welding energy determined by the equations (AWS, 1976):

$$H_{liq} = \frac{f_1 EI}{V}, \quad (3.1)$$

Where f_1 = efficiency of heat transfer, approximately equal to 0,85 for GMAW; E = electric tension in volts (V); I = electrical current in amperes (A); V = welding speed, millimeters by second; H_{liq} = welding liquid energy in joules per mm.

$H_{liq} = 6,23$ J/mm, for the two first passes and $H_{liq} = 12,47$ J/mm, for the remaining passes.

At the Fig. 3.1 is showing the scheme of specimens removal for fatigue crack propagation tests.

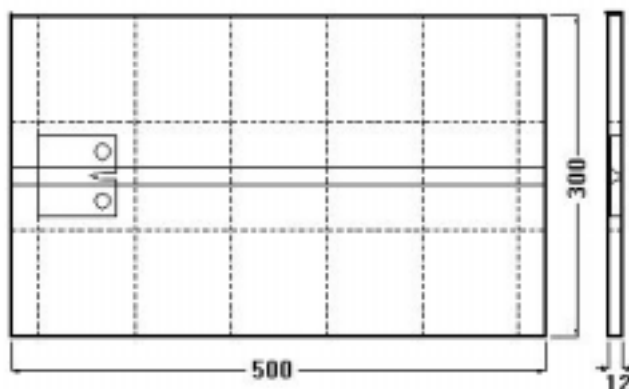


Figure 3.1: Scheme of retired of specimens for fatigue crack propagation tests. 12 mm thickness welded joints. The welds were started at the left of the figure

For the logarithmic linear equation adjust (for to obtain the coefficient C and the exponent n of Paris equation) the Software Excel of the Microsoft was used through regression analysis, and the coefficients and exponents with 95% of confidence were obtained.

The tension properties of the welded joints (HAZ and MZ) were determined by Martins et all (2001) and the means were:

HAZ: Yield stress: $\sigma_e = 403,00 \pm 4,97$ MPa; strength stress: $\sigma_r = 546,33 \pm 6,34$ MPa;

MZ: Yield stress: $\sigma_e = 583,33 \pm 12,81$ MPa; strength stress: $\sigma_r = 652,00 \pm 12,03$ MPa;

The MB properties were determined by Alcântara (2003) as: yield stress: $\sigma_e = 442,9 \pm 7,08$ MPa; strength stress: $\sigma_r = 554,7 \pm 1,1$ MPa;

4. RESULTS AND DISCUSSION

4.1 Graphics of the Tests

On Fig. 4.1 are presented the $da/dN \times \Delta K_{eff}$ curves obtained from fatigue crack propagation tests in several specimens, carried out according ASTM E 647 standard (2000), using the INSTRON, 8802 model equipment of 250 kN capacity. On Fig. 4.1 are presented respectively the $da/dN \times \Delta K$ and $da/dN \times \Delta K_{eff}$ crack propagation curves, for MB01 specimen from BM and on Fig. 4.1 b are presented the fatigue crack propagation curves from BM several specimens.

From an analysis of the crack propagation rate graphics of the BM, it is noticed that the specimens MB02, MB04, presented as with retardation at the crack propagation rate with values of ΔK_{eff} between 30 and 40 MPa \sqrt{m} . This probably is due to micro structural variations on transversal orientation to rolling orientation involving plastic deformation at the crack tip and combined effects of Young modulus E and ratio stress R (Lal, 1996);

On Fig. 4.2 are presented the $da/dN \times \Delta K_{eff}$ graphs of Z2, Z3, (Fig.4.2 as welded) and Z5, Z6 (Fig. 4.2 b, with stress relieve heat treatment) specimens from welded joints with notch located at HAZ.

It is verified, analyzing the graphics from Fig. 4.2, that there is a great scatter of data from one to another specimen, in boot conditions as welded and with stress relieve heat treatment. The test conditions were the same for all four specimens: stress ratio $R=0,1$ and amplitude $A= 4,6$ kN. This can be, probably due to existence of residual stresses before and after the stress relieve heat treatment.

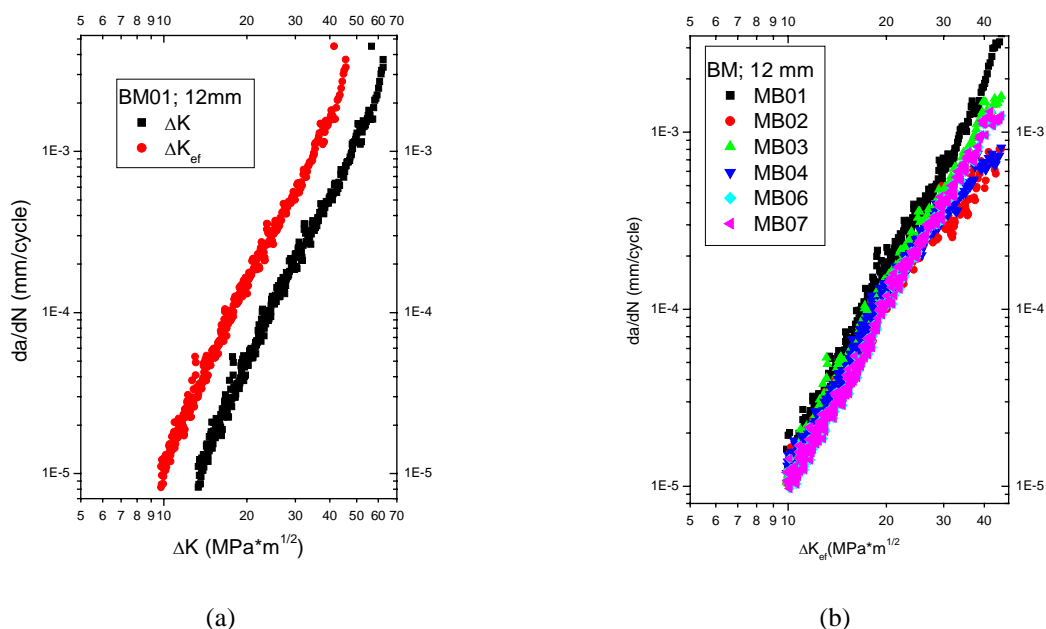


Figure 4.1: Plot of $da/dN \times \Delta K$ and $da/dN \times \Delta K_{eff}$, (a) BM01 specimen; (b) BM01, BM02, BM03, BM04, BM06 and BM07 specimen; plate of 12 mm thickness. $R=0,1$; amplitude 3,6 kN. $R = 0,1$; amplitude 3,6 kN

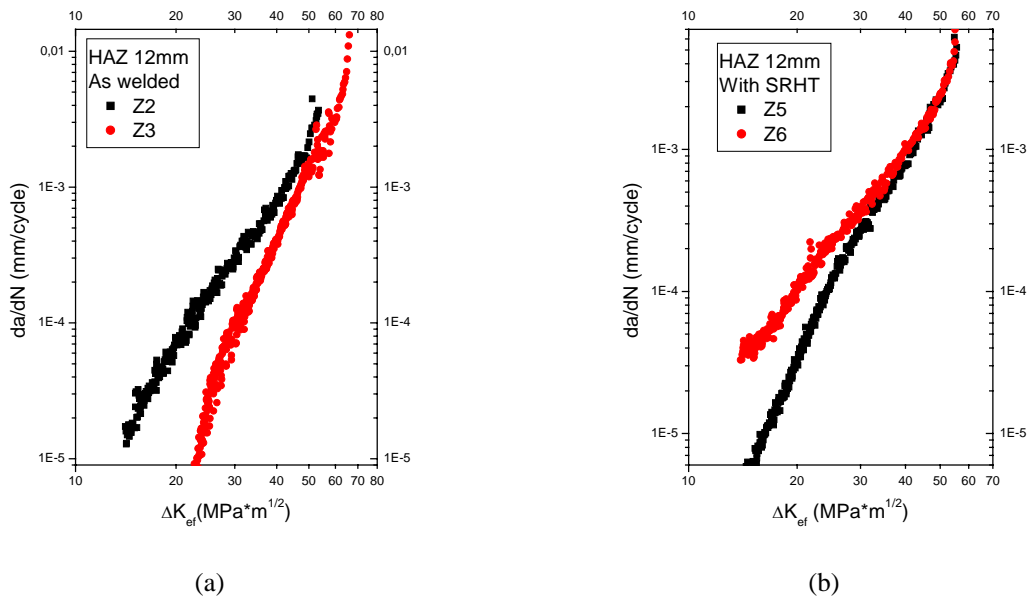


Figure 4.2: Plot of $da/dN \times \Delta K_{eff}$, specimens (a) Z2 and Z3, AW (As Welded) and (b) Z5 and Z6, with SRHT (Stress relieve Heat Treatment) of 12 mm thickness welded joints. $R=0,1$, amplitude 4,6 kN, notch in ZTA

On Fig. 4.3 the fatigue crack propagation graphics of F01, F07 e F11 specimens with notch located at MZ are presented (Fig 4.3 a). These specimens were submitted to tests as welded, with amplitude equal to 4,6 kN load ratio $R=0,1$ and the specimens F13, F14 e F15, with SRHT. The test realized on the specimen F01 started with a crack propagation rate equal to 2×10^{-6} mm/cycle and even so was not determined the ΔK_{th} , the appearance of the crack propagation curve allow to estimate this value. It can see on the graph that specimen F07 presents a great scatter, probably due at an instability of electrical tension that could be caused a lost of regulation of the equipment. It can see to a retardation on the crack propagation rate at ΔK_{eff} near $30 \text{ MPa}\sqrt{\text{m}}$. On the specimen F11, it can see a decreasing at the crack propagation rate at ΔK_{eff} near $50 \text{ MPa}\sqrt{\text{m}}$.

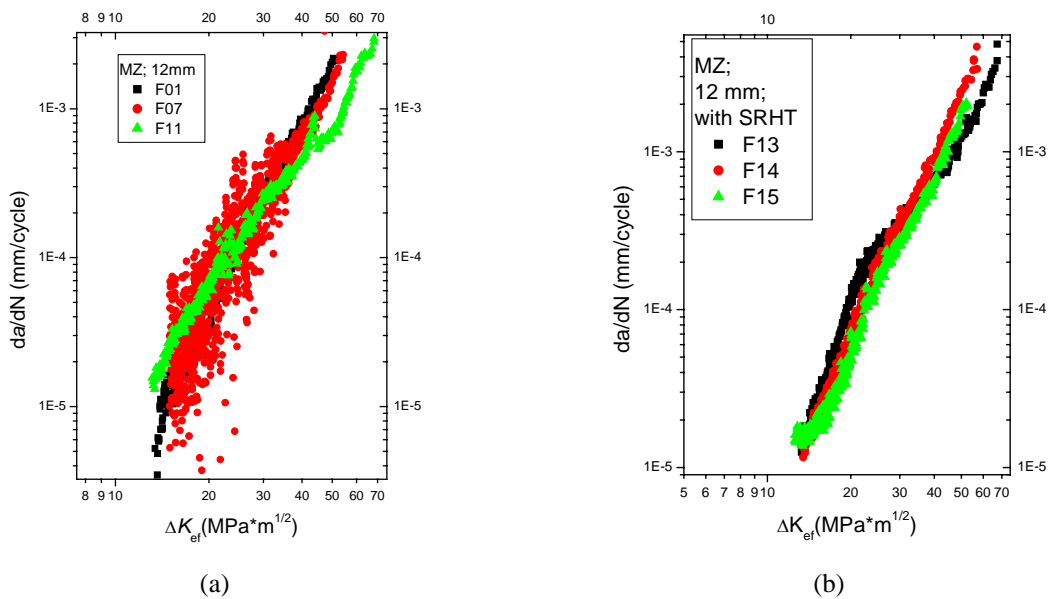


Figure 4.3: Plot of $da/dN \times \Delta K_{eff}$, specimens from 12 mm thickness welded joint notch in MZ, (a) as welded. (F01, F07 e F11); (b) with SRHT (F13, F14 e F15) Amplitude 4,6 kN, $R=0,1$

It can be observed on Fig. 4.3 b the uniformity of the graphics; all present a swift retardation on the crack propagation rate corresponding to a value of 30 MPa \sqrt{m} . This retardation can be due to the existence of compressive residual stresses even so the SRHT.

4.2 Determination of the Coefficients and Exponents Through Regression Analysis

With the purpose of to study the linear region of da/dN versus ΔK_{eff} graph, using the Paris-Erdogan equation, it was fulfilled regression analysis of the resulted data from the tests, to obtain the coefficients (C) and exponent (n) of the Paris equation, with 95% of confidence. From the Eq. 4.1:

$$\frac{da}{dN} = C \times (\Delta K)^n \quad (4.1)$$

Results:

$$\text{Log}\left(\frac{da}{dN}\right) = \text{Log}(C) + n\text{Log}(\Delta K) \quad (4.2)$$

Equation of the type: $Y = A + nX$

Through regression analysis, the coefficients C and exponents n are obtained with the standard error corresponding. The C values are obtained from A values. The ΔK_{eff} values was used to eliminate the influence of ratio R . The values of C and n were grouped according to thickness and test conditions (as welded, stress relieve heat treatment) and the results are presented on Tab. 4.1.

Table 4.1: Values of coefficients C and exponents n of Paris equation, with 95% confidence

Groups	Values of coefficient C			Values of n		
	Mean	95% Inferior	95% Superior			
MB12	4,487 x 10 ⁻⁹	4,235 x 10 ⁻⁹	4,753 x 10 ⁻⁹	3,430	3,411	3,450
Z12(CS)	1,120 x 10 ⁻⁹	6,856 x 10 ⁻¹⁰	1,903 x 10 ⁻⁹	3,486	3,330	3,642
Z12(TTAT)	8,963 x 10 ⁻¹⁰	6,121 x 10 ⁻¹⁰	1,313 x 10 ⁻¹⁰	3,742	3,624	3,859
ZF12(CS)	4,999 x 10 ⁻⁹	4,093 x 10 ⁻⁹	6,105 x 10 ⁻⁹	3,164	3,102	3,226
ZF12(TTAT)	1,595 x 10 ⁻⁹	1,395 x 10 ⁻⁹	1,823 x 10 ⁻⁹	3,559	3,518	3,601
C12	1,567 x 10 ⁻⁹	1,322 x 10 ⁻⁹	1,856 x 10 ⁻⁹	3,442	3,395	3,490

The uniformity of the specimens that were submitted to stress relieve heat results more evident when compared in whole. The difference in the A coefficients can be attributed to the fact that the notch localization is not exactly the same on the several specimens, relatively to microstructure (fine granulation, coarse granulation or region that was submitted to heat treatment) due to subsequent passes.

As can be observed, the coefficient values for the two groups, as welded and with stress relieve heat treatment, indicate that the specimens as welded present propagation rates inferior to specimens that were submitted to stress relieve heat treatment. It is probably due the fact that the stress relieve heat treatment had relieve the compressive residual stresses favoring the crack propagation at the corresponding region.

Despite of the dispersion between the graphics corresponding to F07 and F11, it can be notice a god agreement for the two graphics that indicate a tendency to a major difference on ΔK_{th} and on K_c . The specimen F07 indicates a ΔK_{th} lower and a K_c greater relatively to F11 that shows an opposite tendency.

The stress relieves heat treatment realized on the specimens with notch on MZ presented a positive effect on the util life. The first exhibited a value of 953166 cycles without stress relieve heat treatment and the second, a value of 1.074073 cycles with stress relieve heat treatment (obtained by numerical integration using the Paris equation), a increase about 11%. The calculus were made for two specimens submitted to stress cycles and in the same conditions ($R=0,1$ and amplitude 4,6 kN).

In a master dissertation realized by Silva (2000), using the same material, the same welding procedure, 12 mm thickness were realized ΔK_{th} tests for BM, HAZ and MZ. He has obtained for a same stress ratio a ΔK_{th} inferior for the BM and superior for the MZ, the value of HAZ remaining between the two values. It was verified on his work that at higher loads ratios the ΔK_{th} were lower. The crack propagation tests on his work were realized with stress ratio of 0,3 and 0,7. It was observed too that the ΔK_{th} decrease with the increase of the stress ratio R but at the region II of propagation there is coincidence of the results.

Barson and Rolfe (1999) present typical values of coefficients and exponents of Paris equation for ferritic-perlitic steels C and n respectively equals to 3,6 x 10⁻¹⁰ and 3. The Os values obtained on this work are in concordance with the values presented by Barson and Rolfe and with the values obtained by Marco Filho (2002)

respectively: $C = 4,6 \times 10^{-9}$ and $n = 2,82$, for $R = 0,1$, although on his work the steel employed was the API 5L Grad X-65 steel, a steel ferritic-perlitic also.

5. CONCLUSIONS

The fatigue crack propagation results realized using specimens with notch located at the BM, HAZ and MZ allow to the following conclusions:

- 1) The tests made on the BM specimens with notch according the L-T orientation presented a small retardation, probably due to structural at the transversal orientation to the rolling orientation, that involves plastic deformation at the crack tip and combined effects of Young modulus and ratio stresses;
- 2) The crack propagation evolution is more homogeneous at the BM and less homogeneous at the HAZ in as welded condition. This major dispersion and no-homogeneity at the HAZ is probably due to compressive residual stresses that delay the crack propagation locally;
- 3) On specimens with notch at the HAZ and that were submitted to stress relieve heat treatment, the obtained results were more homogeneous than the specimens as welded. This was because the residual stress relieve that after relieved were distributed in a homogeneous form at the crack propagation front;
- 4) The fatigue crack propagation results on the specimens with notch located at the MZ, resulted in a behavior similar to the
- 5) The Paris equation coefficients, obtained by regression analysis, permit to furnish a confidence interval (95% in this work).

6. REFERENCES

TARA, F L. de, (2003). Comportamento do crescimento de trinca por fadiga de um aço do tipo USI-SAC-50 laminado a quente em diferentes espessuras. Dissertação de mestrado. Pontifícia Universidade Católica de Minas Gerais. Belo Horizonte, MG.

AMERICAN SOCIETY FOR TESTING AND MATERIALS ASTM E 647 (2000). Standard Method for Measurement of Fatigue Crack Growth Rates. Philadelphia.

AMERICAN SOCIETY FOR TESTING AND MATERIALS. ASTM E 1823, (2000). Standard terminology relating to fatigue and fracture testing. Philadelphia.

AMERICAN WELDING SOCIETY, (1982). Carbon and Low Alloy Steels, in Welding Handbook, vol 4, Metals and Their Weldability. Seventh Edition, Miami, Fl.

ANDERSON, T. L., (1995) Fracture Mechanics. Fundamentals and Applications. CRC Press, 2^a ed., Texas, USA.

BARSON, J. M., ROLFE, S. T., (1999). Fracture and fatigue control in structures. Applications of fracture mechanics. 3^a ed. Prentice Hall, Inc., Englewood Cliffs, New Jersey.

HERTZBERG, R., (1989). Deformation and fracture mechanics of engineering materials. 3^a ed. John Wiley & Sons. New York, NY.

KANNINEN, M. F. e POPELAR, C. H., (1985). Advanced fracture mechanics. Oxford University Press. USA.

KUMAR,R.; SINGH, K., (1995). Influence of stress ratio on fatigue crack growth in mild steel. Engineering Fracture Mechanics, Vol. 50, N^o 3, pp. 377-384.

MADOX, S. J.; CURNEY, T. R.; MUMMEY, A. M. and BOOT, G. S. (1978). Na investigation of the influence of applied stree ratio on fatigue crack propagation in structural steels. Research report 72/1978, Welding Institute.

MARCO FILHO, F., (2002). Propagação de trincas de fadiga em juntas soldadas circunferenciais de aço API 5L grau X-65 para utilização em rizers rígidos. Tese de Doutorado. Escola de Engenharia da Universidade Federal do Rio de Janeiro. Rio de Janeiro, RJ.

MARTINS, G. DE P., CIMINI, C. A e GODEFROID. L. B., (2001) Influence of welding planar defects in the fracture toughness of structural steel. Preliminary testings 16th International Conference on Structural Mechanics in Reactor Technology, Washington.

MASUBUCHI, K., (1970). Control of distortion and shrinkage in welding. WRC - Bulletin; April, 1970.

SILVA, J. G. A., (2001). Avaliação comportamental de juntas soldadas de um aço estrutural do tipo SAC 50 sob fadiga. Dissertação de mestrado. Escola de Minas de Ouro Preto. Curso de Pós-graduação em Engenharia Civil. Universidade federal de Ouro Preto.

SURESH, S. (1998) Fatigue of materials. Cambridge University Press, 2^a ed., New York, NY, USA.